Blake Tolmie 33078913

Rylie Obrien 13658230

Abstract

Finite element analysis was applied to a truss structure that supports an elevated billboard. The point joint assumption was determined to not be valid for this analysis; therefore, a frame element analysis was deemed most appropriate. The Euler-Bernoulli beam assumption was determined to be valid for this analysis as the addition of shear deformation did not have a significant influence on the structure. To achieve a factor of safety of 2.5 the maximum wind speed the structure would be required to be rated for was found to be 230km/h.

Introduction

This report investigates applying finite element analysis to a truss structure that supports an elevated billboard. The structure contains 10 elements with elements 1 constrained to the first fixed support and elements 2 and 3 constrained to the second fixed support. The validity pin-joint assumption for the structure is tested using point loads comparing a bar element model and a frame element model. The wind loading is then applied to the frame model, the sensitivity to Euler-Bernoulli Beam Bending Assumption is then tested by comparing the Euler-Bernoulli and Timoshenko formulations.

Method

The structure was initially modeled using bar elements. This system contained 10 degrees of freedom as shown in appendix A. This approach uses the pin-joint assumption, which allows for free rotation and restricts translation.

The structure was also simultaneously modeled using frame elements. This system contained 15 degrees of freedom as shown in appendix B. This approach assumed ridged joints, which restricts both rotation and translation.

For each element of the structure a local and global stiffness matrix was generated.

Assembly matrices were then generated based on the free body diagrams as shown in appendix A & B. The frame element assembly matrices are as shown in Table 1. The bar element was set up in a similar, except with the degrees of freedom resisting rotation removed.

Table 1 Assembly Matrices for the Frame Element Model

A1	A2	A3	A4	A5
np.array([[0,0,0,1,0,0], [0,0,0,0,1,0], [0,0,0,0,0,1], [0,0,0,0,0,0], [0,0,0,0,0,0], [0,0,0,0,0,0], [0,0,0,0,0,0], [0,0,0,0,0,0], [0,0,0,0,0,0], [0,0,0,0,0,0], [0,0,0,0,0,0], [0,0,0,0,0,0], [0,0,0,0,0,0], [0,0,0,0,0,0], [0,0,0,0,0,0]])	np.array([[1,0,0,0,0,0], [0,1,0,0,0,0], [0,0,1,0,0,0], [0,0,0,0,0,0], [0,0,0,0,0,0], [0,0,0,0,0,0], [0,0,0,0,0,0], [0,0,0,0,0,0], [0,0,0,0,0,0], [0,0,0,0,0,0], [0,0,0,0,0,0], [0,0,0,0,0,0], [0,0,0,0,0,0], [0,0,0,0,0,0], [0,0,0,0,0,0]])	np.array([[0,0,0,0,0,0], [0,0,0,0,0,0], [0,0,0,1,0,0], [0,0,0,0,1,0], [0,0,0,0,0,1], [0,0,0,0,0,0], [0,0,0,0,0,0], [0,0,0,0,0,0], [0,0,0,0,0,0], [0,0,0,0,0,0], [0,0,0,0,0,0], [0,0,0,0,0,0], [0,0,0,0,0,0], [0,0,0,0,0,0], [0,0,0,0,0,0]])	np.array([[1,0,0,0,0,0], [0,1,0,0,0,0], [0,0,1,0,0,0], [0,0,0,1,0,0], [0,0,0,0,1,0], [0,0,0,0,0,1], [0,0,0,0,0,0], [0,0,0,0,0,0], [0,0,0,0,0,0], [0,0,0,0,0,0], [0,0,0,0,0,0], [0,0,0,0,0,0], [0,0,0,0,0,0], [0,0,0,0,0,0], [0,0,0,0,0,0]])	np.array([[1,0,0,0,0,0], [0,1,0,0,0,0], [0,0,1,0,0,0], [0,0,0,0,0,0], [0,0,0,0,0,0], [0,0,0,1,0,0], [0,0,0,0,1,0], [0,0,0,0,0,1], [0,0,0,0,0,0], [0,0,0,0,0,0], [0,0,0,0,0,0], [0,0,0,0,0,0], [0,0,0,0,0,0], [0,0,0,0,0,0], [0,0,0,0,0,0]])
A6	**A7**	**A8**	**A9**	**A10**
np.array([[1,0,0,0,0,0], [0,1,0,0,0,0], [0,0,1,0,0,0], [0,0,0,0,0,0], [0,0,0,0,0,0], [0,0,0,0,0,0], [0,0,0,0,0,0], [0,0,0,0,0,0], [0,0,0,1,0,0], [0,0,0,0,1,0], [0,0,0,0,0,1], [0,0,0,0,0,0], [0,0,0,0,0,0], [0,0,0,0,0,0]])	np.array([[0,0,0,0,0,0], [0,0,0,0,0,0], [1,0,0,0,0,0], [0,1,0,0,0,0], [0,0,1,0,0,0], [0,0,0,0,0,0], [0,0,0,0,0,0], [0,0,0,0,0,0], [0,0,0,1,0,0], [0,0,0,0,1,0], [0,0,0,0,0,1], [0,0,0,0,0,0], [0,0,0,0,0,0], [0,0,0,0,0,0]])	np.array([[0,0,0,0,0,0], [0,0,0,0,0,0], [0,0,0,0,0,0], [0,0,0,0,0,0], [0,0,0,0,0,0], [1,0,0,0,0,0], [0,1,0,0,0,0], [0,0,1,0,0,0], [0,0,0,1,0,0], [0,0,0,0,1,0], [0,0,0,0,0,1], [0,0,0,0,0,0], [0,0,0,0,0,0], [0,0,0,0,0,0]])	np.array([[0,0,0,0,0,0], [0,0,0,0,0,0], [0,0,0,0,0,0], [0,0,0,0,0,0], [0,0,0,0,0,0], [1,0,0,0,0,0], [0,1,0,0,0,0], [0,0,1,0,0,0], [0,0,0,0,0,0], [0,0,0,1,0,0], [0,0,0,0,1,0], [0,0,0,0,0,0], [0,0,0,1,0,0], [0,0,0,0,0,1]])	np.array([[0,0,0,0,0,0], [0,0,0,0,0,0], [0,0,0,0,0,0], [0,0,0,0,0,0], [0,0,0,0,0,0], [0,0,0,0,0,0], [0,0,0,0,0,0], [0,0,0,0,0,0], [0,0,0,1,0,0], [0,0,0,0,1,0], [0,0,0,0,0,1], [1,0,0,0,0,0], [0,1,0,0,0,0], [0,0,1,0,0,0]])

Individual element contributions to the global stiffness matrix were calculated and then summed together for the overall global stiffness matrix.

The global forcing vector Q was applied to solve for overall structural deflections, q. For the comparison of the bar elements and frame elements a point loading vector was applied as the global forcing vector. For the wind loading analysis a uniformly distributed load was applied on the 2 appropriate elements, which was used as the global forcing vector.

To solve for reaction loading the element nodal forces in global co-ordinates were calculated, each reaction force was solved by using the following formulas:

$$Reaction\ Force\ 1 = F^{1}_{1-3}$$

$$Reaction\ Force\ 2 = F^{2}_{4-6} + F^{3}_{1-3}$$

The element nodal forces in local co-ordinates were calculated to allow for stress calculations. Finding the total normal stress was calculated by the following formula:

$$\sigma_{\text{total}} = \frac{|N|}{A} + \frac{|M|\,c}{I}$$

where N is axial force, M is local bending moment, A is cross-sectional area, c is distance to outer fiber, and I is the second moment of area.

Discussion and Results

The Deflection for tip of structure was found using the overall structural deflections from the solved displacement vector, as shown in Table 2. The frame model shows a 2 milliradian rotation clockwise resulting in a significant decrease of deflection in both the X and Y axis. This suggests that the pin-joint assumption is not ideal to use for this structure.

Table 2 Point Loading Deflection of Tip of Structure

	Bar	Frame
X(mm)	13.29	5.78
Y (mm)	13.02	1.01
Moment (mrad)	N/A	-2.00

The reaction forces were obtained using the element nodal forcing vectors in global coordinates, as shown in Table 3. Reactions in the bar element model x axis were far larger

than expected, this was due to the inability to resist rotation. This suggests the pin joint assumption is not appropriate for this analysis.

Table 3 Point Loading Reaction Forces

	Reaction force from element 1		Reaction force from element 2 & 3	
	Bar	Frame	Bar	Frame
X (N)	-114465	-2375.82	54464.79	-57624.2
Y (N)	228380.2	-286200	-228380	286200.2
Moment (Nm)	N/A	4722.033	N/A	9077.787

The axial forces experienced by the elements were obtained from the element nodal forcing vectors in element coordinates, as shown in Table 4.

Axial loading shows much larger peak axial forces on bar elements when compared with frame elements. This may be partially explained by the bar elements only considering axial forces. This is a limitation regarding purely checking axial forces as the bending forces within the frame element are ignored and misrepresenting the actual force the element is experiencing.

The structure for both models was in equilibrium with both Y axis values counteracting each other and the X axis has a reaction of -60kN which is counteracting the 60kN from the applied point loads.

Table 4 Point Loading Element Axial Forces

Element	Bar (kN)	Frame (kN)
1	140.8	-286.2
2	221.1	143.2
3	-371.5	153.9
4	0.0	1.2
5	-1929.8	-41.3
6	-3641.9	-111.0
7	-2165.1	144.1
8	30.0	28.8
9	-290.9	-37.0
10	608.2	39.8

Bar element stress was calculated by taking the axial stress, with a pin joint assumption there was no bending stress. Frame element stress was calculated by summing the axial stress and bending stress, as shown in Table 5. Due to no forces being applied along the elements themselves the largest bending stress would be located at the points connecting the elements. Both ends of each element were checked for the greatest moment to be used for the stress calculation of that element.

The peak stress from the bar element was found to be 810 MPa, due to the nodal forces in local co-ordinates for the bar element having 1 dimension this force is not located on a specific point on the element. The peak stress from the frame element was found to be 87.9 MPa located at the reaction point which connects to the ground from element 1.

Elements 5, 6, and 7 in the bar model are overestimated by a factor greater than 10 when compared to frame model. This can be used to determine that the use of the pin-joint assumption is not appropriate for this analysis.

Table 5 Point Loading Element Absolute Normal Stresses

	Normal Stress (MPa)	
Element	bar	frame
1	31.3	87.9
2	49.2	52.4
3	82.6	60.3
4	0.0	27.8
5	429.2	19.7
6	810.0	31.7
7	481.6	45.0
8	6.7	18.5
9	64.7	10.5
10	135.3	9.3

The bar model uses pin-joint assumption simplifies analysis. It has led to inaccurate reaction forces and overestimated axial forces leading to a significant overestimation of peak normal stresses. Frame offers a more accurate solution with a slight increase in complexity.

The bar model overemphasizes reinforcing the center of the structure, overlooking critical stress points at the bottom of the structure. The frame model recognizes that the greatest stresses occur at the bottom of the structure.

To calculate the low-zone wind max stress magnitude and location within the structure, the Part-1 point loads were removed and replaced by the wind-pressure UDL with load

$$w = p * d$$

where p was static pressure p = 0.61 Pa, and d was depth of the sign d = 8m. This UDL was applied to vertical elements 5 and 9 with the assumption that the wind would act normally to the sign face.

For each element in the structure, and for UDL members at the point in the member where the shear is zero, the total normal stress was calculated. It was important for the UDL members to also calculate the total normal stress at the point where the shear force was zero, since for these members the maximum total normal stress may not occur at the node ends. This was unlike the other elements in the structure where the maximum total normal stress of the element was at the node ends.

The maximum normal stress of 34.9 kPa for the structure was in element 1 in Table 6. This was expected since element 1 sits below the wind-loaded elements 5 and 9, so it carries the accumulated shear from the UDLs and resists the resulting overturning couple at the base. There were also very small deflection components at the top of the structure, meaning the structure can likely withstand higher wind loads.

Table 6 Low-Zone Wind Load Results

Parameter	**Value**
Maximum normal stress in frame (Pa)	34,852.96
Element with maximum normal stress	Element 1
Deflection at top of frame (m, m, rad)	$(5.21\times10^{-6}, 3.95\times10^{-7}, -4.55\times10^{-7})$

The maximum wind loading and speed was determined by iteratively increasing wind speed until the maximum stress exceeded the yield stress of 350 MPa divided by a safety factor of 2.5. From Table 7 the structure was rated for a maximum wind speed of 230km/h. The deflection components at the top of the frame were small relative to the structure height, confirming the small angles assumption, and that the stiffness of the sign was adequate at high wind load conditions.

The support reactions in Table 8 show that the vertical forces carried most of the loading, which was expected since the UDL was acting on the vertical elements. The moments at the supports reflect the fixity at the base and how the frame resists overturning. The

horizontal reactions were much smaller in magnitude than the vertical forces, but they still played an important role in resisting the overturning couple from the applied wind.

Table 7 Maximum Wind Load Results

Parameter	**Value**
Maximum normal stress in frame (Pa)	1.40×10^{8}
Element with maximum normal stress	Element 1
Maximum wind speed (m/s) & (km/h)	63.90 & 230.06
Deflection at top of frame (m, m, rad)	(0.02093, 0.00159, −0.00183)

Table 8 Maximum Wind Load – Support Reactions

Support	$\boldsymbol{F_x\ (N)}$	$\boldsymbol{F_y\ (N)}$	$\boldsymbol{M_z (Nm)}$
Support 1	−2,942.59	−468,636.59	6,963.57
Support 2	−95,069.41	468,636.59	14,459.84

The maximum wind loading case was re-analysed with Timoshenko beam elements to account for shear deformation. The shear effects from Timoshenko caused a 0.3% increase in x deflection, and a 3.5% reduction to rotation outlined in Table 9. This determined that the small angles assumption was valid. In comparison, there was a 10% increase in the horizontal force of support 1, and a small decrease of 4-5% in the moments at both supports in Table 10. These changes were within acceptable limits.

Overall, the addition of shear deformation did not have a significant influence on the structure. The Euler-Bernoulli beam assumption was valid for this analysis, and the exclusion of shear deformations did not compromise the accuracy of the results.

Table 9 Comparison of Maximum Wind Load Results – Euler–Bernoulli vs. Timoshenko

Parameter	**Euler–Bernoulli Result**	**Timoshenko Result**	**Difference**
Maximum wind speed (m/s)	63.90	63.90	0 %
Deflection at top (Δx, m)	0.02093	0.02099	+0.3 %
Deflection at top (Δy, m)	0.00159	0.00159	≈0 %
Rotation at top (θ_z, rad)	−0.00183	−0.00176	−3.5 %

Table 10 Support Reactions – Euler–Bernoulli vs. Timoshenko

Reaction Component	Support	Euler–Bernoulli	Timoshenko	Difference
Horizontal Force, $F_x\ (N)$	1	−2,942.6	−2,640.9	+10 %
	2	−95,069.4	−95,371.1	−0.3 %
Vertical Force, $F_y\ (N)$	1	−468,636.6	−469,649.9	−0.2 %
	2	468,636.6	469,649.9	+0.2 %
Moment, $M_z(Nm)$	1	6,963.6	6,674.0	−4.2 %
	2	14,459.8	13,736.1	−5.0 %

Conclusion

The point joint assumption was determined to not be valid for this analysis. The distribution of forces from bending significantly impacted the stresses experienced by each element. The Euler-Bernoulli beam assumption was determined to be valid for this analysis as the addition of shear deformation did not have a significant influence on the structure. To achieve a factor of safety of 2.5 the maximum wind speed the structure would be required to be rated for was found to be 230km/h.

Appendix A - Diagram global degrees of freedom for bar

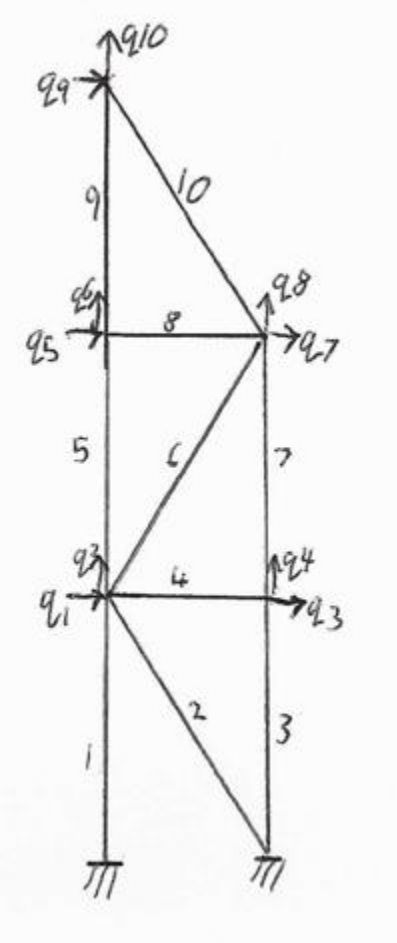

FBD for bar

Element 4 and 8

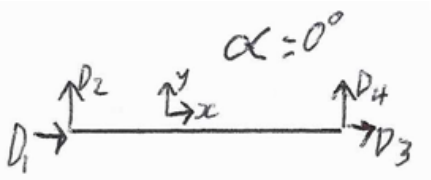

Element 1,3,5,7 and 9

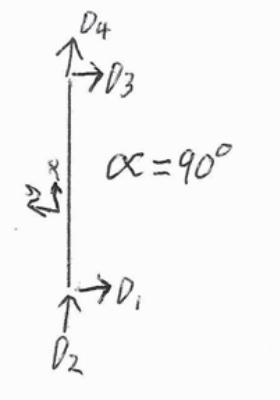

Element 6

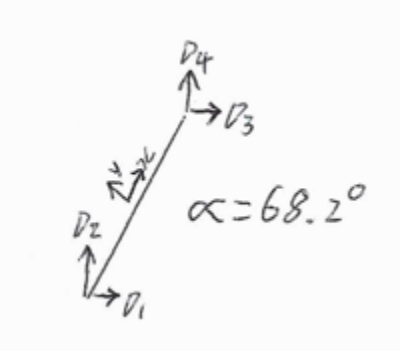

Element 2 and 10

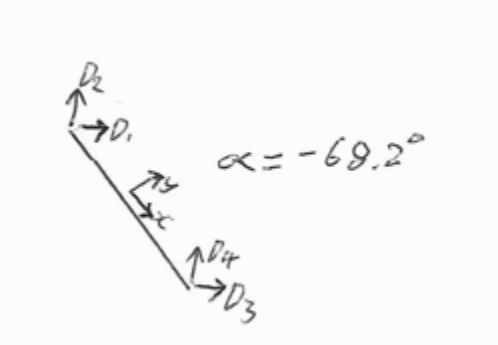

Appendix B - Diagram global degrees of freedom for frame

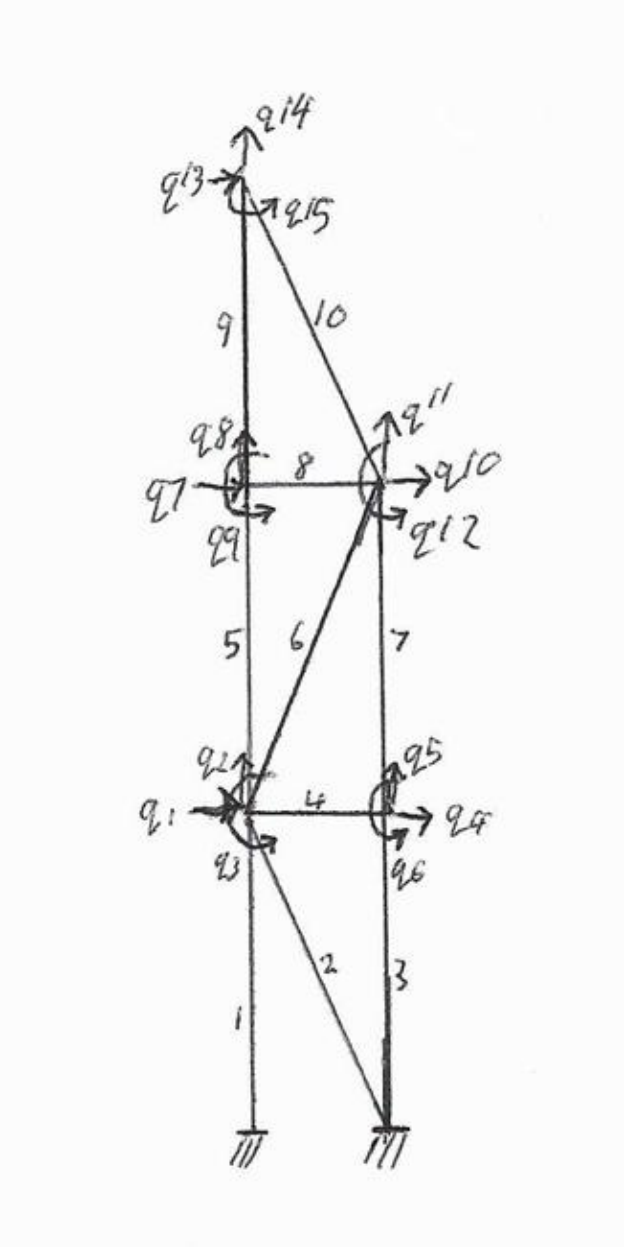

FBD for frame

Element 4 and 8

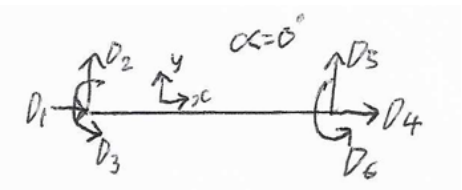

Element 1,3,5,7 and 9

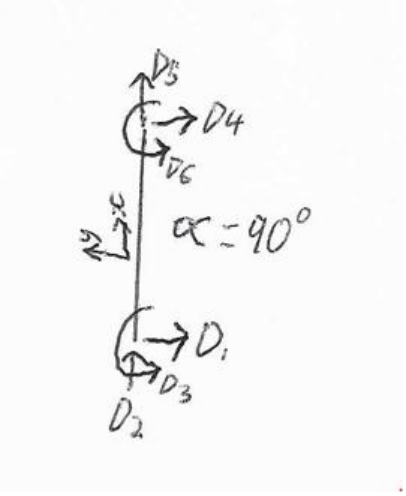

Element 6

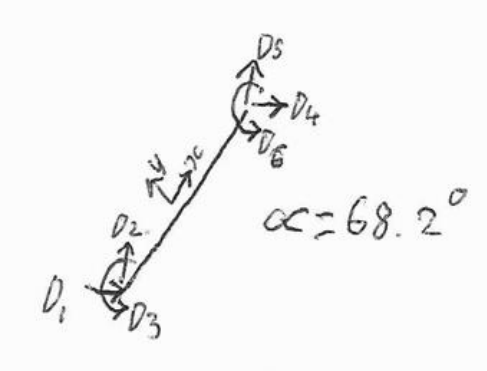

Element 2 and 10